Journal of Manufacturing Processes 68 (2021) 1767–1783

Contents lists available at ScienceDirect

Journal of Manufacturing Processes

journal homepage: www.elsevier.com/locate/manpro

Regional temperature control in ceramic injection moulding: An approach based on cooling rate optimisation

Maria Floriana Bianchi [a], Andreś A. Gameros [a,*], Dragos A. Axinte [a], Stewart Lowth [a], Aleksander M. Cendrowicz [b], Stewart T. Welch [c]

[a] Rolls-Royce UTC in Manufacturing and On-Wing Technology, University of Nottingham, Advanced Manufacturing Building, NG8 1BB, UK
[b] Rolls-Royce Plc, High Temperature Research Centre, Unit 2, Airfield Drive, Ansty Business Park, Coventry CV7 9RD, UK
[c] Rolls-Royce Plc, Precision Casting Facility, Wilmore Road, Derby DE24 9BD, UK

ARTICLE INFO

Keywords:
Ceramic injection moulding
Rapid thermal cycling
Regional mould temperature control
Cooling rate optimization

ABSTRACT

The injection moulding of ceramic components with uneven wall thickness presents challenges due to differential cooling rates developing in the injected parts, which cause premature solidification of the feedstock at thin features and lead to detrimental defects, worsening in components from green to sintered states. To cope with this, suitable mould thermal control approaches have to be selected and validated, as current control methods are based on the achievement of a uniform cavity surface temperature, which is not tailored to such complex geometries. In this work, a novel thermal control system is proposed, based on regional mould temperatures, implemented with the use of Peltier modules, which locally and independently heat and cool different cavity features according to their thickness. The regional temperature profiles are optimised over time with the use of a coupled Finite Element - Particle Swarm Optimisation (FE-PSO), to achieve uniform cooling rates throughout the moulded components. The performance of this approach is compared to both constant ambient mould temperature and Rapid Heat Cycle Moulding (RHCM) techniques, which instead aim at achieving uniform temperatures throughout the mould cavity surface. Results show that the novel proposed method, based on regional temperature control and uniform cooling rates, promotes the simultaneous solidification of features with a 10-times difference in surface-to-volume ratio. Due to this, in terms of components quality, the novel method brings the advantages of higher dimensional control and reduction of differential shrinkage compared to the other analysed approaches, thus increasing the capability to use injection moulding to manufacture ceramic components characterised by non-uniform wall thickness.

1. Introduction

Ceramic Injection Moulding (CIM) is a widely used mass production process consisting of three main steps: injection moulding, debinding and sintering. In order to decrease shear forces during the injection process, and subsequently reduce internal residual stresses in green (pre-firing) components, and to limit tool wear when using highly abrasive ceramics, lowering the injection pressure is an effective technique, for which the process variant "Low Pressure Ceramic Injection Moulding" (LPCIM) is employed [1]. While in the conventional CIM process pressures over 100 to 200 bar are operated, these are reduced down to 5 to 10 bar, together with melt temperatures, which are usually kept below 100 °C in LPCIM.

Despite its advantages, the employment of these process parameters brings about challenges in feature replication capability for thin-walled and micro components [2]. To cope with these issues, mould temperature has been proven to be the most significant parameter to ensure replication capability and dimensional accuracy for features having aspect ratios [3]. Therefore, a technique known as "Rapid heat cycle moulding" (RHCM) is often used and implemented through steam [4,5,6], consisting of a first increase of cavity temperature during filling to keep the feedstock viscosity low (thus enhancing feature replication capability and weld line formation), and then a fast cool down of the die-tool [7]. High investments in cooling technologies are required for complex thermal control systems which need to guarantee fast and uniform cooling of the injected components to ensure that both the mould and subsequently the part are cooled down to a suitable ejection temperature quickly enough to achieve industry-standard cycle times.

* Corresponding author.
E-mail address: andres.gameros@nottingham.ac.uk (A.A. Gameros).

https://doi.org/10.1016/j.jmapro.2021.06.069
Received 16 November 2020; Received in revised form 19 June 2021; Accepted 25 June 2021
Available online 15 July 2021

Moreover, when moulding complex-shaped parts, straight-drilled cooling channels are usually not capable to achieve an even mould cavity temperature during the process; therefore, conformal cooling channels to the component shape are often used [8]. This implies an even more complex and expensive mould design and development process, often requiring moulds finished by advanced manufacturing techniques (e.g. electropolishing, [9]) for a high-quality surface finish [10]. Moreover, the mould complexity is increased due to the optimisation of the heating and cooling elements location or temperature to guarantee a uniform heat transfer to and from the cavity surface.

In this respect, studies have been carried out to optimise heating/cooling elements configurations and subsequently mould temperatures, using different methods. A novel machine learning training method was developed by Finkelday [11] to optimise mould temperature, along with other process parameters, in relation to component quality. A novel approach, based on a heat conduction inverse problem was proposed by Agazzi [12] to optimise cooling channel geometry. Metaheuristics optimisation has also been used to optimise the design of heating and cooling channels: Wang [13], Xiao and co-workers [14] optimised the layout of steam heating/cooling channels and electric heater locations respectively, using coupled Particle Swarm Optimisation (PSO) and Finite Element Method (FEM) to minimise cycle time with constraints on maximum temperature difference and Von Mises stresses in the cavity. This class of global optimisation methods is particularly useful in such complex design problems, with unknown cost functions and a large search space; when compared to other approaches, such as the Genetic Algorithm, PSO has been proven to converge more quickly to the optimal solution [13], which is of high importance to allow for reasonable computation time when solving problems whose solution needs to be calculated through FEM. Despite the relevance of these pieces of work in developing heating and cooling methods, the reviewed studies mainly focus on the injection moulding of plastic components following the design-for-mouldability guidelines imposing constant wall thickness. This is not always applicable to ceramic parts, as the geometry of some components having strict functional requirements cannot be changed to enhance mouldability (as it happens, for example, for investment casting ceramic cores). Moreover, state of the art tool scaling practices may become unsuitable for these complex geometries as warpage due to improper heating and cooling approaches might not be prevented. Looking at the injection of these geometrically complex ceramic parts, having features of uneven thickness, through the LPCIM process, two main limitations can be found in the analysed literature.

The first limitation is linked to the fact that current studies base the heating/cooling system optimisation on cavity temperature uniformity. This may not be a suitable approach in the case of parts having features with different surface-to-volume ratios, such as ceramic cores used for the investment casting of hollowed turbine blades [15]. In these components, non-uniform cooling and dissimilar solidification rates during injection moulding result in warpage and cracking defects [16], hence, to address these issues, tailored thermal control approaches (e.g. regional heating and cooling) need to be developed. Local mould heating and cooling methods have been proposed in the literature, firstly by Kim [17], who presented the idea of a novel low-thermal-inertia mould, containing thermoelectric modules to enable the local heating and cooling of the cavity: the study proved the use of Peltier technologies for the thermal control of injection moulds, but did not propose any strategy or approach for thermal control or optimisation. An approach based on regional temperature control has been presented by Nian et al. [18]: this method successfully reduces temperature-induced part warpage by controlling cooling channels temperature according to how the component will deform at different cross sections, based on their neutral axis. However, the study does not present any specific algorithm for the determination of the optimal local temperatures and does not consider a RHCM approach, which is necessary in order to achieve complete filling of components having thin features through LPCIM.

The second limitation relates to the analyses on the effects of the proposed systems on parts quality, as they have been mainly restricted to surface appearance and to macroscopic defects, such as sink marks and warpage [19]. Some microstructural analyses have been performed on both unfilled and fibre-filled polymers, to correlate the effect of RHCM on tensile and impact strength to weld line morphology and fibre orientation at merging flow-front locations [20]. On the other hand, when injecting ceramic feedstocks, complex microstructural phenomena such as particle packing and orientation arise due to the influence of mould temperature [21], arise in addition to other mechanisms occurring in polymer moulding: the combination of these phenomena cause defects and adverse microstructures in green parts, which often result in detrimental cracking after debinding and sintering. This brings about further challenges when injecting components having uneven wall thickness with LPCIM. Despite the relevance of these phenomena, coupled conformal cooling and RHCM have not been employed in literature regarding CIM and, to the best of authors' knowledge, no study accounted for the effects of optimised heating and cooling conditions on moulded ceramic components.

Based on the literature, strong limitations exist in developing optimal heating and cooling systems for the injection moulding of components having uneven wall thickness, both because of the lack of optimisation strategies that take into account uneven cooling rates in the part and for restricted understanding on how different approaches affect components microstructure. Therefore, the present work aims at developing and demonstrating a novel thermal control system for LPCIM consisting of regional heating and cooling of the mould cavity, based on an optimisation of cooling rates within the moulded part. The novel mould tool with regionally controlled temperature was designed and manufactured using thermoelectric (Peltier) elements to heat and cool the mould and their temperatures were independently controlled based on the results from a coupled Finite Element (FE)-PSO optimisation. The proposed approach is not only validated in terms of efficiency to respect industry-standard cycle times, but also compared to the conventional isothermal and RHCM approaches for its effect on part quality both at the macrostructural and microstructural levels.

2. Novel mould and temperature control concepts

As previously stated, this work includes the joint development of a mould tool, locally heated and cooled, and of its control approach. This is based on an optimisation, with the objective to minimise cooling rate gradients in moulded parts having differential wall thickness. In this section, the mould and the control approach concepts will be described and discussed.

The mould design can be introduced by taking into account a generic component with features having different thicknesses (Fig. 1a), and, for simplicity, symmetric along the separation plane of the mould (i.e. the interface between the two mould plates). The die-tool with local temperature control is equipped with thermoelectric (i.e. Peltier) modules located at a fixed distance from the cavity surface, one per each feature (Fig. 1b). Peltier elements have a uniform temperature throughout their face and can be used to locally heat and cool each cavity feature. One or more temperature sensors are placed between the Peltier surface and the mould cavity (measuring T_{P1} and T_{P2} shown in Fig. 1b), in order to implement an independent temperature control for each thermoelectric element.

While, in the RHCM approach, temperature control is based on achieving a uniform mould cavity surface temperature (i.e. $T_{1A} = T_{2A}$ in Fig. 1c), the novel thermal control approach is based on minimising thermal gradients within the parts (i.e. $\dot{T}_{1B} = \dot{T}_{2B}$ in Fig. 1d). Therefore, because of the component geometry symmetry, it is based on achieving a uniform temperature in the centre of the part. In order to fulfill this objective, since features of different thicknesses cool at diverse rates, the temperature of each Peltier needs to be adjusted throughout the IM process, as explained in the example cycle of Fig. 2.

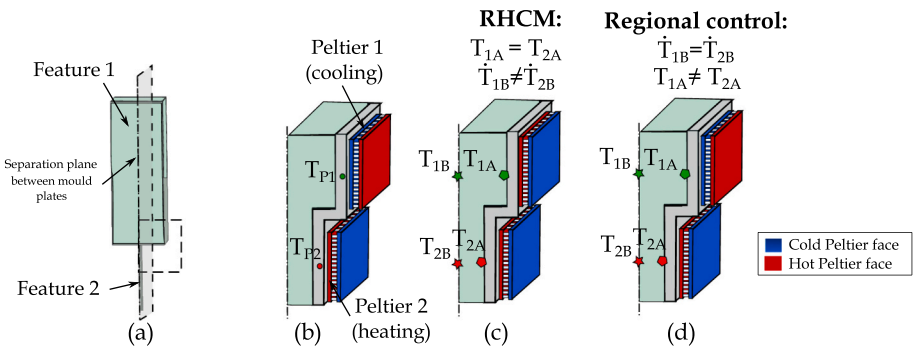

Fig. 1. Concept of the novel thermal control system. (a) Generic component, isometric view. (b) Schematics of Peltier configuration and positioning, showing the independent control for the two features and the location of temperature sensors for closed-loop control of the thermoelectric modules. (c) Schematics of the control approach for RHCM. (d) Schematics of the novel regional control approach. Note: Whole Peltier modules are larger than those displayed, as they occupy the whole feature thickness.

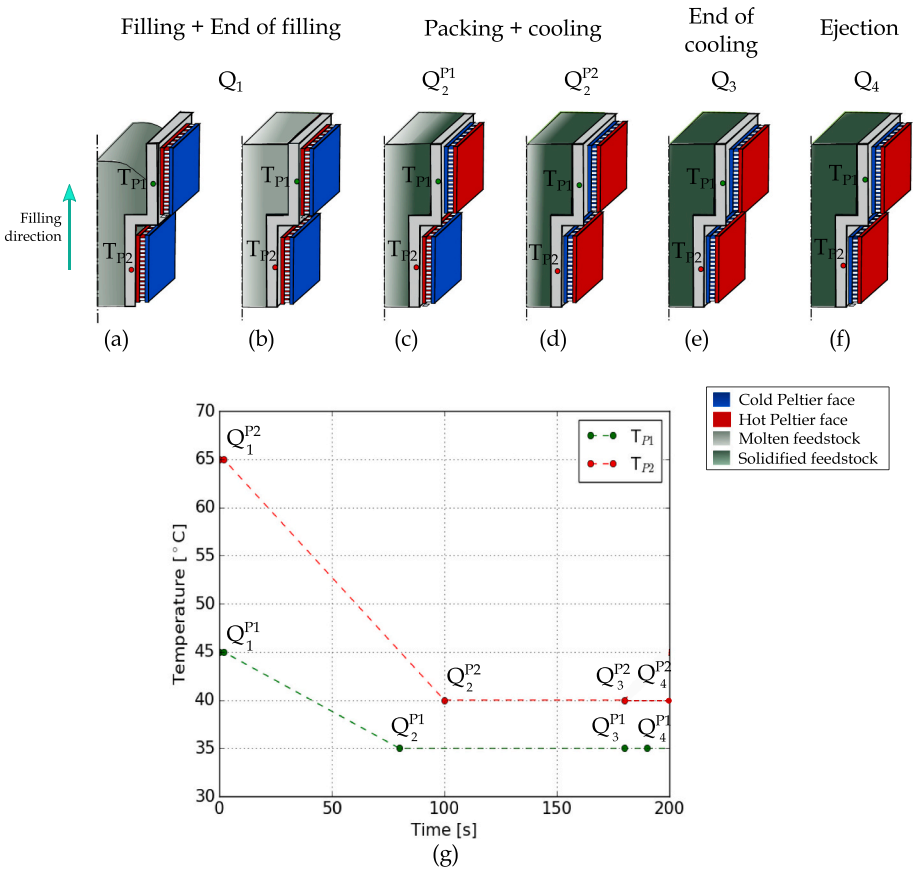

Fig. 2. Example temperature cycle using the novel approach. (a) Filling stage. (b) End of filling. (c) Packing phase, Peltier 1 switches from heating to cooling. (d) Packing phase, Peltier 2 switches from heating to cooling. (e) End of cooling phase. (f) Ejection phase. (g) Thermal profile of the two Peltier modules shown in the schematics.

Considering the generic component previously described, with features having different thicknesses, injected in a way that the feedstock has to flow from a thin (Feature 2) to a thick feature (Feature 1), each Peltier will have an imposed temperature profile throughout the process. One of the main advantages in employing Peltier modules is to enable local heating and cooling, without the need of changing physical configuration, as the face in contact with the mould can be inverted from heating to cooling, just by swapping the direction of the electric current passing through the element. In this way, the temperature of each Peltier can be independently controlled throughout the process, in order to achieve uniform cooling rates in the part. Therefore, the role of the associated thermal control model and optimisation is to compute cooling rates inside the part for different combinations of Peltier temperature profiles, through a transient thermal FE model. Based on this, for each thermoelectric element, the optimal profile is computed with the objective of minimising heating and cooling rate gradients throughout the part, during the whole injection moulding process.

3. Materials and methods

This section outlines the experimental methodology used for the validation of the regional thermal control system, which is defined based on two main areas. First, the feedstock material is presented alongside a description of the experimental setup, control system and the process parameters employed on the CIM trials. Secondly, the strategy to characterise the effect of the novel system on the macro- and micro-structure of the components is presented.

3.1. Materials and experimental setup

A ceramic feedstock (Fig. 3) containing silica (SiO_2) and zircon ($ZrSiO_4$) was employed, with the two compounds being 80% and 20% of the powder loading respectively (by weight). The feedstock has similar characteristics to those usually employed for the injection moulding of aerospace ceramic cores [22].

Particles are elongated in shape and mixed within a binding blend of paraffin wax and ethylene-vinyl acetate (EVA) to achieve a volumetric solid loading of 70% (≈ 85% in weight). The maximum solid loadings (≈ 71% in volume) were measured by the feedstock manufacturer using a pycnometer density-based method [23].Ceramic platelets have a heterogeneous particle size distribution ranging from sub-micron particles, up to 200 μm in the long axis direction; the material has its glass transition temperature (T_g) at 45 °C and melting point at 62 °C (both measured through differential scanning calorimetry), while its specific heat and thermal conductivity (at 25 °C) are 1200 J/(Kg*K) and 0.7 W/(m*K). The viscosity behaviour of the feedstock, based on experimental data measured by the supplier, is shown in Fig. 4.

Since the geometry of the workpiece highly affects cooling rates in injection mould-ing, the selection of sample parts with distinct surface-to-volume ratios is essential. Moreover, simplicity of the parts is needed to successfully isolate the root cause of any defect that may be detected in injected parts. Therefore, two components characterised by straight channels with variable cross sections were designed (Fig. 5) and specifically conceived to have the following geometrical and process-related properties:

- Uneven wall thickness: sample parts are made of distinct channels having constant wall cross sections with dissimilar surface-to-volume (S/V) ratios (the thin features have approximately 10 times higher S/V ratio than the thick ones).
- Filling patterns going *from-thick-to-thin* and *from-thin-to-thick* features.

These sample geometries were injection moulded on an experimental setup comprising an injection unit, a mould unit and a control unit. The injection unit (Fig. 6) comprises a double action pneumatic cylinder with a 50 mm bore and maximum operating pressure of 10 bar, used to replicate a plunger type injection moulding machine used in industrial environments for LPCIM. The feedstock is pushed by the piston from an aluminium tank to the mould cavity through a nozzle, while the aluminium tank is heated up with two closed-loop controlled Peltier modules to maintain a constant melt temperature.

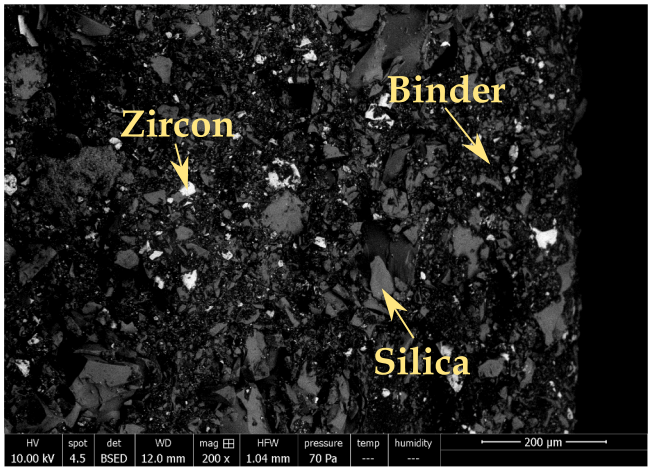

Fig. 3. Micrograph of the feedstock (green state) used for the study. (For interpretation of the references to colour in this figure legend, the reader is referred to the web version of this article.)

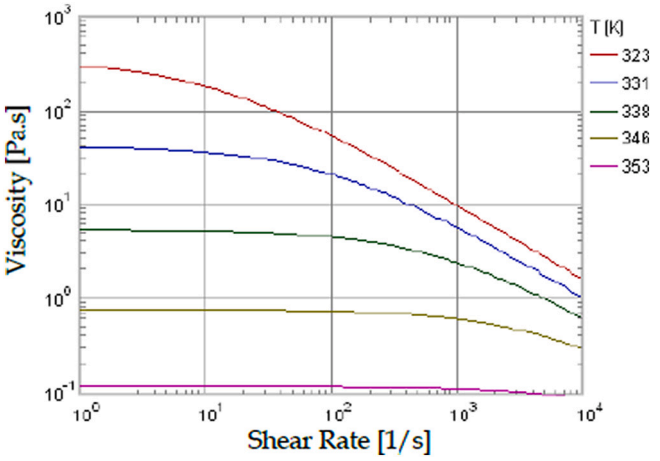

Fig. 4. Viscosity profile, as a function of shear rate and temperature, for the feedstock used in the study.

The mould unit consists of the novel die-tool (Fig. 7a), designed with four aluminium (Al 7075-T651) mould plates (1); 12 thermoelectric modules (2) were placed below or above (for bottom and top plates respectively) each feature, with 3 mm distance between the Peltier face and cavity surface (Fig. 7d).

Separate mould plates (two bottom and two top) were designed for the two cavities, in order to allow for the drilling of thermistor housings between the features and the thermoelectric modules (Fig. 7d). To insulate the mould from the heatsink side and enhance Peltier efficiency, two glass-fibre filled resin sheets (3–4) were placed between the mould and base plates (5–6). Two large heatsinks (7–8) were located at the two extreme top and bottom sides to allow for heat dissipation.

Housings for cylindrical inserts to block and deviate the material flow were machined to allow for four different injection configurations (Fig. 8): filling of Cavity A (Step-part) with Single Sprue (SS), filling of Cavity B (Draft-part) with SS, filling of Cavity A with Double Sprue (DS), filling of Cavity B with DS.

The control unit was designed to independently regulate the Peltier modules temperatures, through a proportional control implemented in an Arduino. This was, in turn, connected to three driver shields with H-bridges, used to deliver the appropriate power to the thermoelectric elements with a Pulsed-Width-Modulation (PWM) signal, depending on the temperature read by the thermistors. Sensors were also placed within the cavity to measure temperature inside the part and validate the thermal model.

In order to evaluate the novel proposed approach, three sets of injection moulding experiments were carried out, each corresponding to a specific thermal control method, with different temperature profiles per each feature (thin or thick), as shown in Fig. 9: isothermal (ambient mould temperature), RHCM and regional control (optimised case).

For each set of trials, three repetitions were carried out for every cavity and injection configuration (with a total number of 36 injections). A preliminary series of trials (not reported here, as out of the scope of this study) was made in order to select suitable levels of injection pressure and flow rate to allow for maximum cavity filling without material flashing out of the mould, given the available clamping force (10.5 kN): based on this, injection pressure was set at 5 bar and the maximum flow rate was 12 cm^3/s, while melt temperature was kept constant at 75^o C.

3.2. Characterisation methods

To assess the performance of the proposed thermal control approach, the moulded parts macro- and micro-structural quality outcomes were studied and related to the heat transfer phenomena occurring during the

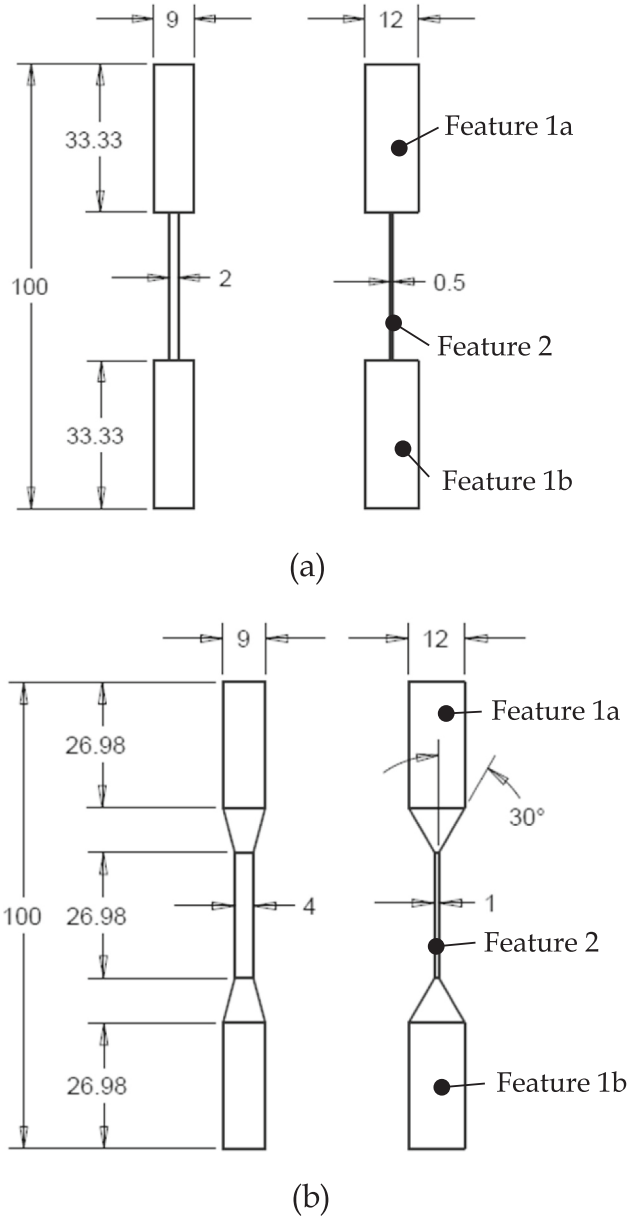

Fig. 5. Sample components. (a) Component A: "Step-part". (b) Component B: "Draft-part".

process. First, feature replication capability was visually assessed; then dimensional accuracy was evaluated by measuring the injected parts with an Alicona InfiniteFocus optical microscope, to evaluate differences in shrinkage among parts moulded with the different methods. A fixture was used to align the samples to a reference ground plane and the top surfaces of the samples were scanned to compare their relative heights. Weld lines morphology and phase separation at components surface were measured using the Alicona InfiniteFocus optical microscope and a FEI Quanta 650 Environmental Scanning Electron Microscope (SEM) in low vacuum mode (at a chamber pressure of 70 bar). To evaluate differences in particle packing and orientation, samples were then sliced with a brittle cut and the SEM was used to analyse their cross sections. In order to compare the performances of the novel regional approach to other state-of-the-art thermal control methods, these analyses were performed on the same components moulded using constant ambient mould temperature and RHCM. The analysis is done exclusively on green bodies parts as post sintering results are considered outside the scope of the present work since defects on fired components may not be due to the injection moulding process but to suboptimal; debinding/sintering [24].

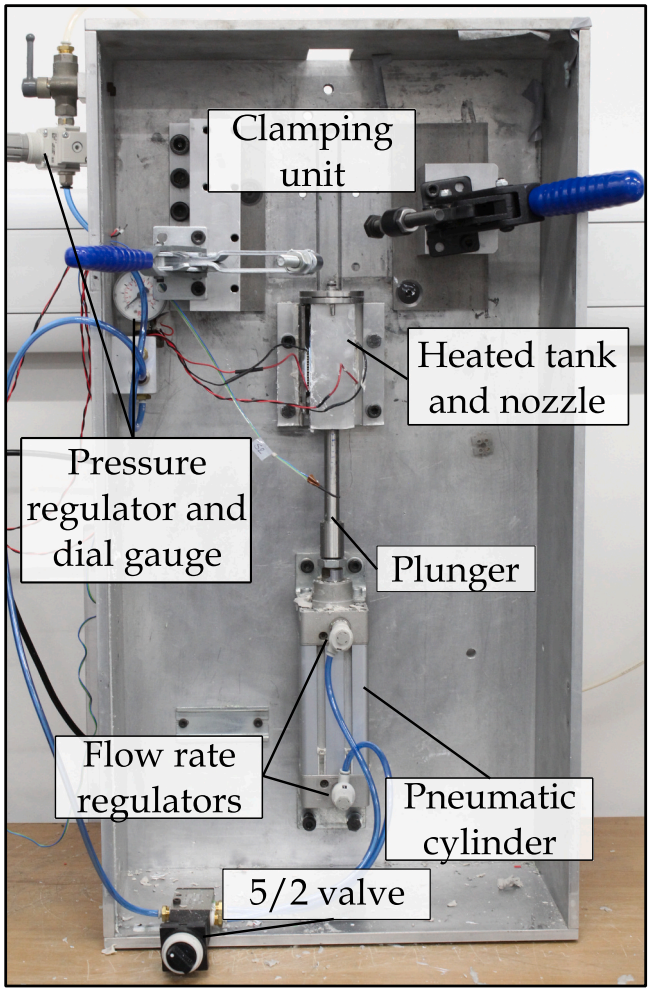

Fig. 6. Laboratory rig used as injection unit to validate the novel mould tool prototype with regional temperature control.

4. Thermal control model and optimisation

The development and demonstration of the mould with regional temperatures was supported by a thermal control model, used to determine optimal temperature distribution along the part throughout the moulding cycle, which was implemented using a coupled Finite Element - Particle Swarm Optimisation (FE-PSO) method (Fig. 10).

The PSO optimises the temperature profile of each Peltier in the regionally controlled mould, to minimise thermal gradients in the centre of the part throughout the injection moulding process. A FE transient heat transfer model of the packing and cooling phases of the IM process was implemented in ABAQUS, in order to predict the temperature distribution and cooling rates inside the part, needed to compute the objective function of the PSO. Moreover, a heat and mass transfer simulation of the filling process, implemented in the software Moldex3D, was used in order to predict temperature distribution in the part at the end of the IM filling stage that was employed as initial condition to the thermal model in ABAQUS.

In the following sections, the optimisation will be firstly described, including the main variables, optimisation functions, constraints and PSO parameters. Then, the setup of both the filling and the "packing-cooling" models (in Moldex3D and ABAQUS respectively) will be shown and discussed.

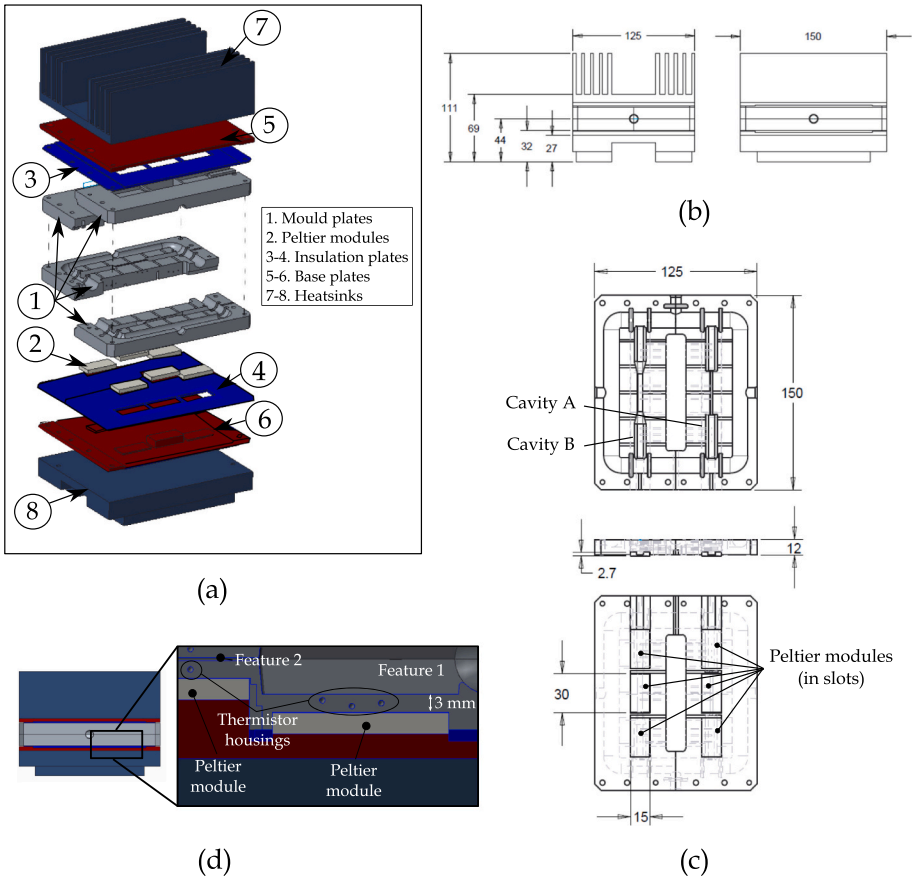

Fig. 7. Prototype of the novel mould tool. (a) Exploded view of the assembly. (b) Main dimensions. (c) Mould cavity, main dimensions. (d) Cross section of the mould, showing Peltier modules and thermistor housings locations.

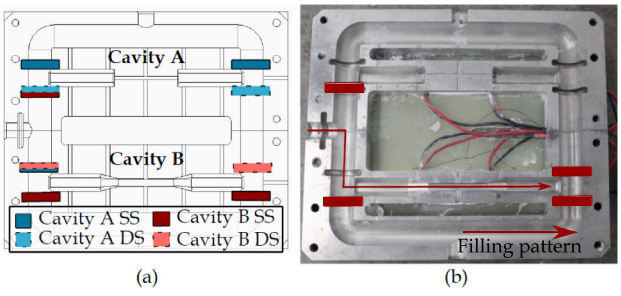

Fig. 8. Mould unit, injection configurations. (a) Schematics of possible injection configurations (b) Example configuration for Cavity B (Draft-part) SS.

4.1. Optimisation of mould temperatures

As previously stated, the objective of the implemented optimisation is to find the temperature profiles over time $T(t)$ per each region of the mould (i.e. per each Peltier module) which minimise thermal gradients in the part throughout all the injection moulding process stages. To achieve this, the definition of the optimisation variables is based on a subdivision of the whole process window. Considering a generic point Q with coordinates (t, T), corresponding to a temperature T at an instant of time t during IM, the process window can be divided into four phases (Fig. 11), going from points $Q_1 - Q_2$, $Q_2 - Q_3$ and $Q_3 - Q_4$ of the graph respectively.

The optimisation variables are then defined as the coordinates (i.e. time and temperature) of each control point: the temperature profile between each couple of control points $Q_i - Q_{i+1}$ is assumed to be linear. Since a different temperature profile needs to be accounted for each of the Peltier modules in the mould, the optimization strategy needs to account for a total of $8P$ variables, where P is the number of the Peltier modules (i.e. thermal regions) on the mould.

The use of this approach for constructing the optimisation enables a wide problem exploration, however, it implies the use of a high number of variables, which increases the computational time: this is not desirable, especially when a FE simulation has to be solved to compute the fitness function. Therefore, to simplify the problem, both the number and the domain of the optimisation variables have been selected based on the following:

- The initial time, corresponding to the end of injection and the beginning of the packing and cooling phases is the start of the analysis: $t(Q_1) = 0$.
- The initial mould temperature only admits two values (RHCM or ambient): $T(Q_1) = T_{low} \vee T(Q_1) = T_{high}$.
- The final cooling temperature must be lower than the glass transition point of the material binder and was fixed to a value: $T(Q_3) = T_{low}$.
- All the temperature values were bonded to lower and upper limits coincident to the two possible values assumed at the beginning of the analysis: $T(Q_i) = [T_{low}, T_{high}], \forall\, i$.

To account for further process requirements, the following constraints were implemented:

1. The part must be solid at ejection: $T(Q_4) \leq T_{sol}$.
2. Each phase must be completed prior to the starting of the next phase in the process window: $t(Q_i) \leq t(Q_j), \forall\, i, \forall\, j = i + 1$.

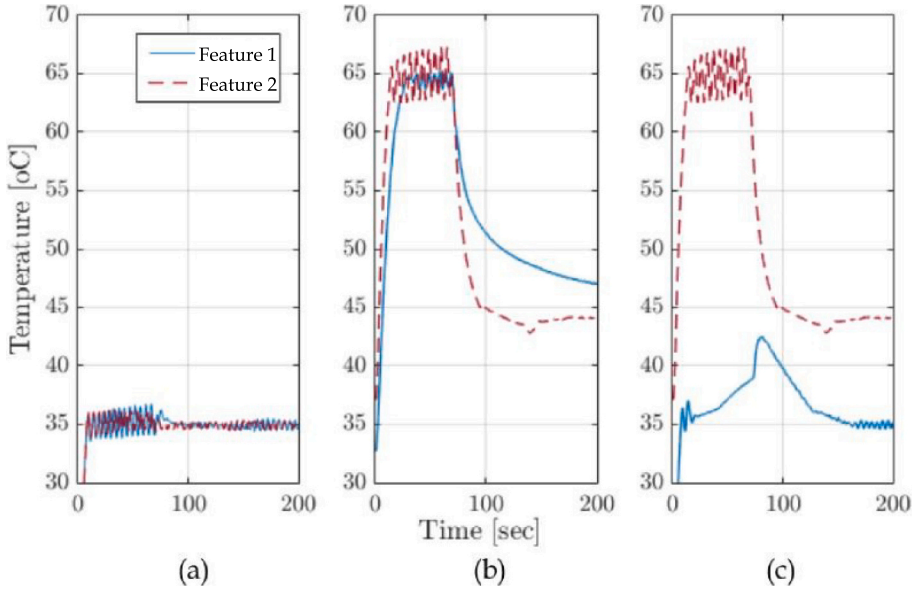

Fig. 9. Example temperature profiles for the three employed thermal control approaches, showing the Peltier temperatures corresponding to the thick (Feature 1) and thin features (Feature 2) of the mould. (a) Ambient mould temperature. (b) RHCM. (c) Regional control approach.

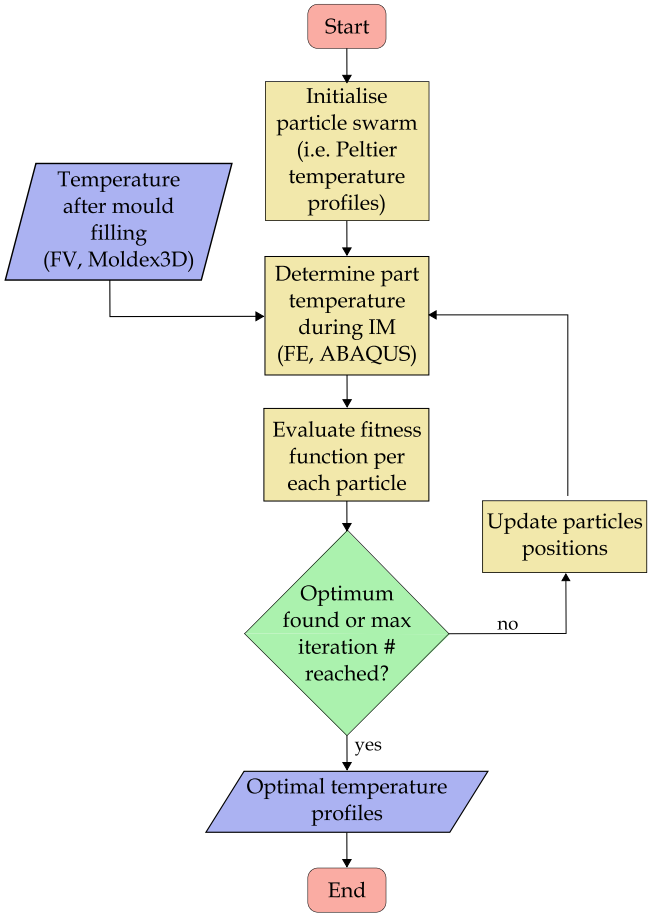

Fig. 10. Flow chart of the thermal control model.

3. Mould temperature at the thin feature needs to be higher than the feedstock T_g to allow for mould filling: $T(Q_1) \geq T_g$.

Moreover, the swarm initialisation includes the choice of the following parameters, whose values are displayed in Table 1::

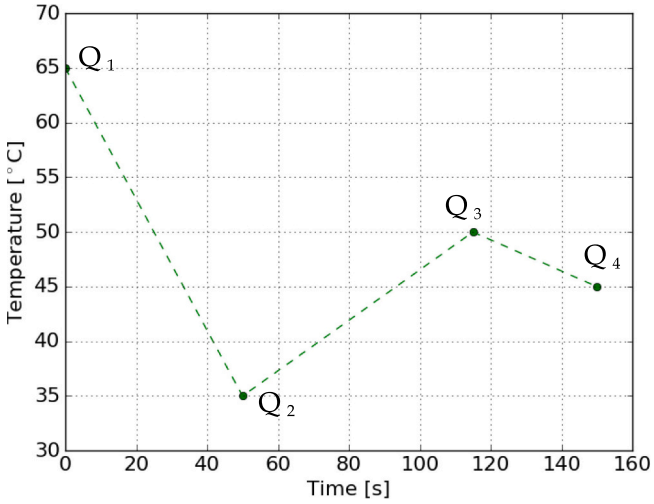

Fig. 11. Example process window used for FE-PSO variable definition, for a single Peltier. Note: A different set of parameters is valid per each Peltier.

- Swarm size n: the number of particles within the swarm, where each particle corresponds to an instance of the optimisation variables.
- Maximum number of iterations K.

Table 1
PSO parameters used for the performed optimisation.

Parameter	Value
T_{low} [°C]	35
T_{high} [°C]	65
T_{sol} [°C]	47
n	50
K	100
ω	0.5
c_1	0.5
c_2	0.5

- PSO coefficients (ω, c_1, c_2) which determine the method of movement within the search space (i.e. how, given the results from all previous iterations, the algorithm will update the values/position assumed by the particles in the swarm).

The fitness function f_c, to be minimised with the PSO method, was defined as:

$$f_c = \alpha\left(\Delta\dot{T}_{max} + \Delta\dot{T}_{ave}\right) + \beta T_{bool} + \gamma t_{step} \quad (1)$$

where $\Delta\dot{T}_{max}$ and $\Delta\dot{T}_{ave}$ are respectively the maximum and the average differences in cooling rates in the centre of the thin and thick features of the channels, throughout the packing and cooling phases; T_{bool} is a boolean variable used to satisfy constraint number 1 (i.e. the part needs to be solid at ejection); t_{step} is the total packing and cooling time, corresponding to the cycle time of the process; α, β and γ are weighting coefficients. Both $\Delta\dot{T}_{max}$ and $\Delta\dot{T}_{ave}$ were minimised to account for peaks in cooling rates as well as mean shifts. At each PSO iteration, the fitness function value is calculated per each particle: to do this, values for cooling rates were determined using two numerical simulations of the IM process, which are described in the following section.

4.2. Numerical modelling of the injection moulding process

The first developed model is a mould filling simulation, carried out using the injection moulding Finite Element-Finite Volume Method (FEM-FVM) software Moldex3D, from which the temperature distribution throughout the part at the end of filling was mapped and used as an initial boundary condition for the second model, used to simulate the packing and cooling phases, implemented as a FE transient heat transfer analysis in ABAQUS.

For the first simulation, the modelled assembly (Fig. 12) included the part (i.e. the reference geometries shown in Section 3.1), the mould envelope (i.e. the aluminium plates) and the Peltier modules, modelled as solid rectangular plates having a defined temperature.

The heatsinks were not modelled and thermal effects from the face of the thermoelectric cooler in contact with them were neglected, as the two Peltier faces (i.e. the one in contact with the mould and the one in contact with the heatsink) were thermally isolated. The assembly was meshed with tetragonal elements, having minimum seed size of approximately 0.1 mm to ensure a properly refined mesh of the thinnest features (0.5 mm thick). To simulate the filling process, the feedstock viscosity behaviour (as a function of shear rate and temperature) and PVT behaviour were modelled based on experimental data measured by the feedstock supplier, using a Cross-Exp law [25] and a modified Tait model [26] respectively. Heat capacity and thermal conductivity as a function of temperature were also considered, based on measured data from the feedstock supplier. The mould envelope was modelled with

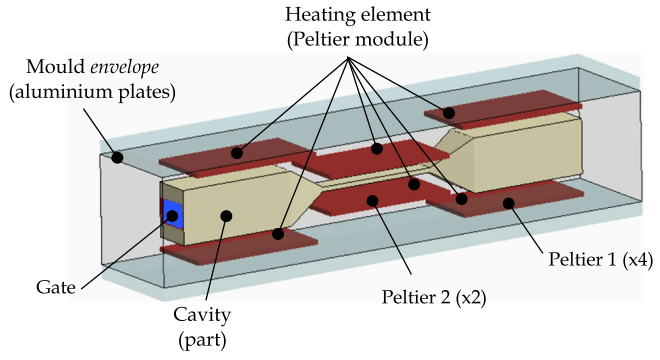

Fig. 12. Assembly modelled in Moldex3D filling simulation, consisting of moulded cavity, mould plates and heating/cooling elements.

Aluminium 7075-T651 density and thermal properties. As for the employed BCs and ICs, the flow rate and injection pressure values reported in Section 3.1 were respectively used as inlet BC and maximum pressure level during mould filling, and the pre-set pressure filling-to-packing switch-over condition was set at the point when nozzle pressure equalised the maximum injection pressure. A no-slip condition was assumed at the mould-part interface. The feedstock inlet temperature was set based on the melt temperature used in the IM experiments, while the Peltier temperatures were imposed according to two different modelled scenarios: (i) all Peltier modules at 65 °C and (ii) Peltier 2 (i.e. the one under the thin cavity) at 65 °C while Peltier 1a and Peltier 1b at 35 °C.

For the second simulation (i.e. the FE model of the cooling stage implemented in ABAQUS), symmetry in load and geometry were used. The assembly included only the moulded part and mould cavity, while the Peltier modules were instead modelled as temperature BCs on the mould bottom (and hence top, for symmetry) surfaces (Fig. 13).

A tetragonal quadratic mesh with minimum seed of 0.1 mm was also constructed for this model, in order to ensure a sufficient number of elements along the thinner features of the mould and cavity. As the simulation is a transient heat transfer model, only the density, thermal conductivity and heat capacity of the ceramic feedstock and of the Aluminium 7075-T651 mould were modelled. An adiabatic BC was imposed at surfaces corresponding to gate locations: this condition was considered under the assumption of simultaneous solidification of the runner features close to the gate location. A thermal conductance BC was employed between the mould and the part, with a value of 1500 W/m^{2}K, of the same order of magnitude with respect to values found in literature [27]. A workflow was implemented in order to automatically feed into the FE simulation both the temperature BCs corresponding to the Peltier thermal profiles (Fig. 11) from the PSO algorithm, and the mapped temperature distribution throughout the part and mould at the end of filling, from the Moldex3D simulation results.

Through these numerical models, part temperature distribution during the whole IM process was determined, and the cooling rates $\Delta\dot{T}_{max}$ and $\Delta\dot{T}_{ave}$ were calculated as time derivative of the average temperature profiles within two node regions in the centre of the part features (Node sets A and B in Fig. 13). Finally, these cooling rates were fed-back to the PSO simulation to compute the optimisation fitness function, also in this case by a developed workflow.

5. Results and discussion

In this section, the results of the performed modelling and experimental work are presented and discussed, as anticipated in Section 3. First the results of the PSO will be presented, along with an analysis of the heat transfer phenomena occurring using the novel developed system and optimised control. In particular, an insight will be given on how the novel and optimised system affects cooling rates and temperature distribution in the part. Moreover, the throughput and thermal efficiency of the designed system will be discussed. Finally, the performance of the novel thermal control system will be evaluated by analysing its effect on the macro- and micro-structural properties of injection moulded green parts.

5.1. Optimisation results and thermal analysis

The optimised Peltier temperature profiles, resulting from the PSO, for the two reference geometries, include the employment of a different control for their thin and thick features, as shown in Fig. 14.

The optimal Peltier profiles include a constant ambient temperature for the Peltier under the thick feature (Peltier 1) and a localised-RHCM approach for the Peltier under the thin feature (Peltier 2). At the end of the process, to ensure safe part ejection, a rise of temperature is also included for both Peltier modules, up to the feedstock T_g.

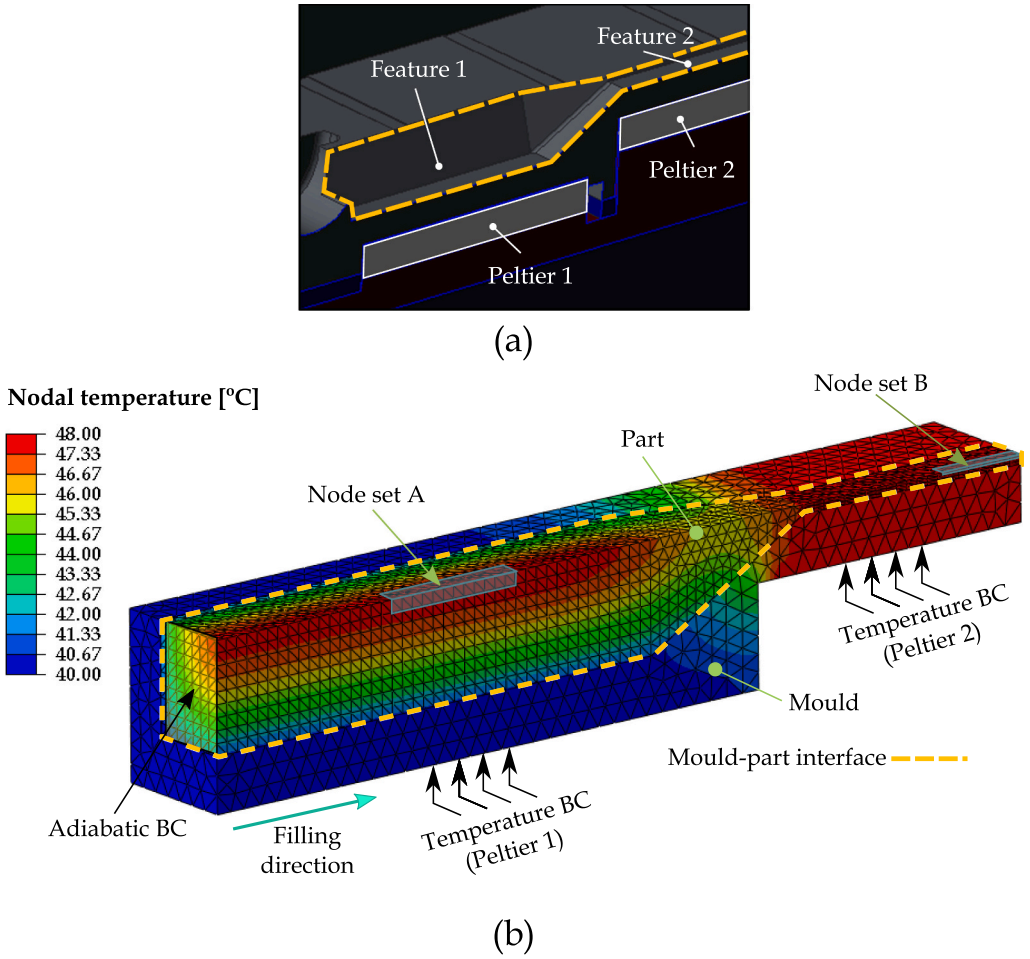

Fig. 13. Example of ABAQUS-modelled assembly (Draft-part) (a) CAD model of the assembly. (b) Schematics of the model setup, showing the used mesh and temperature distribution.

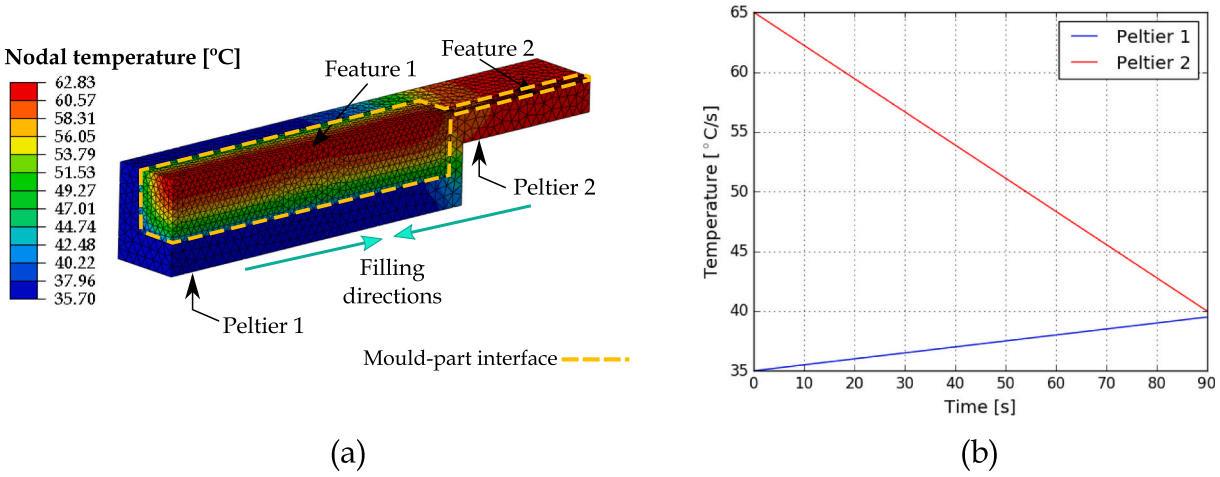

Fig. 14. Results from the thermal control model and optimisation: example for the Step-part in DS configuration. (a) 3D mesh. (b) Optimal Peltier temperature profiles.

Moreover, it is possible to compare the effects on the cooling rates within the part achieved using the optimised regional controlled approach (Fig. 15a and c) to what happens in RHCM (Fig. 15b and d).

First of all, a clear distinction between the two thermal control approaches can be noticed in terms of temperature profiles inside the parts. In the RHCM case (Fig. 15e), the material in the thin feature (Feature 2) solidifies faster than the feedstock in the thick feature (with a difference in solidification time $\Delta t(T_s)$ of approximately 20 s); on the other hand, in the optimal case (Fig. 15f), joint freezing occurs between the two features. Considering the case of single sprue (SS) injection configuration, if the thin feature solidifies faster, the thick feature farther from the gate will not be packed properly during the holding stage (Fig. 16).

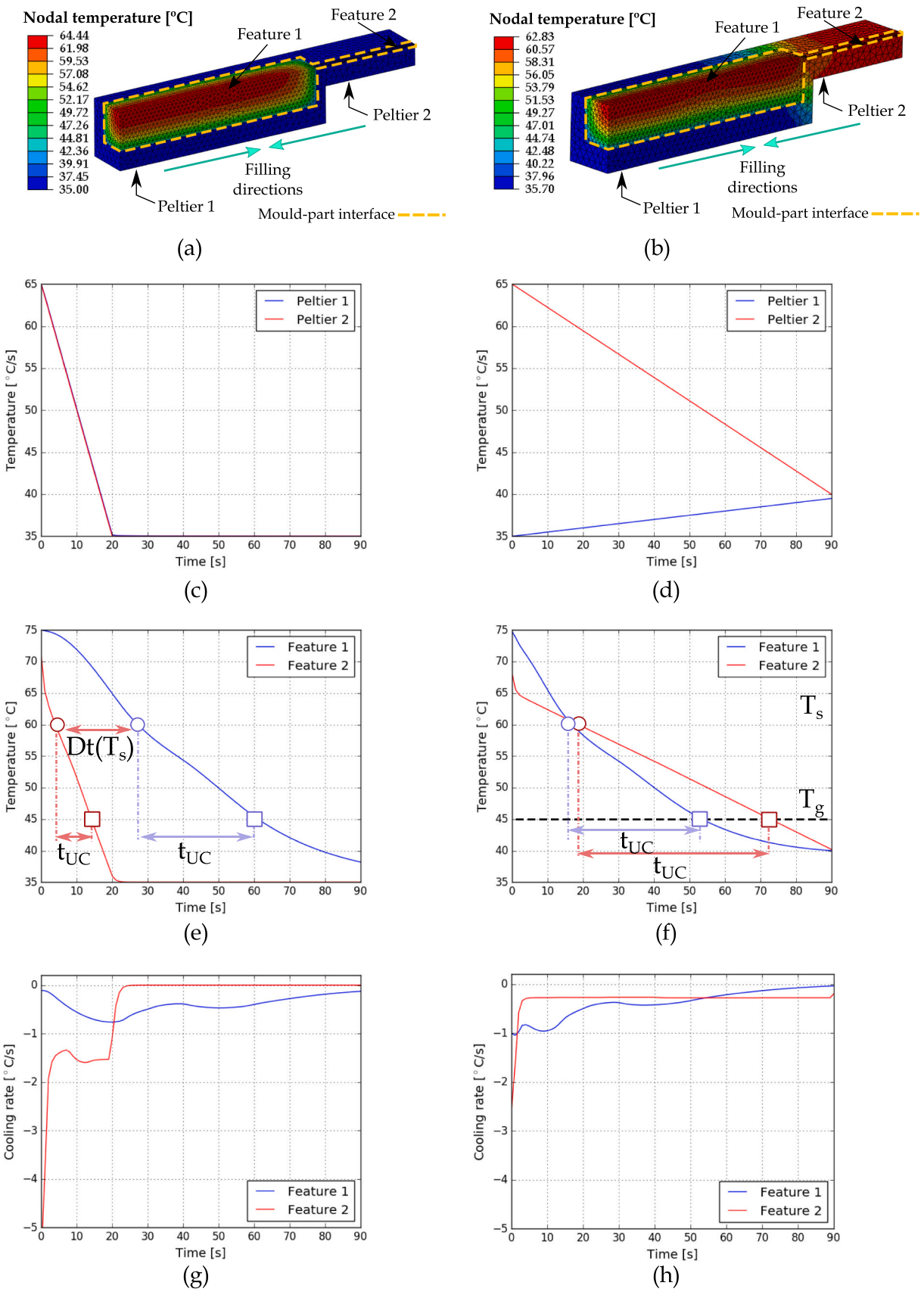

Fig. 15. Results from the thermal control model: example for Step-part in DS configuration. (a) 3D mesh, RHCM. (b) 3D mesh, optimised regional. (c) Peltier temperature profile, RHCM. (d) Peltier temperature profile, optimised regional. (e) Feature cooling rate profile (node sets A and B), RHCM. (f) Feature cooling rate profile (node sets A and B), optimised regional. (g) Feature temperature profile (node sets A and B), RHCM. (h) Feature temperature profile (node sets A and B), optimised regional.

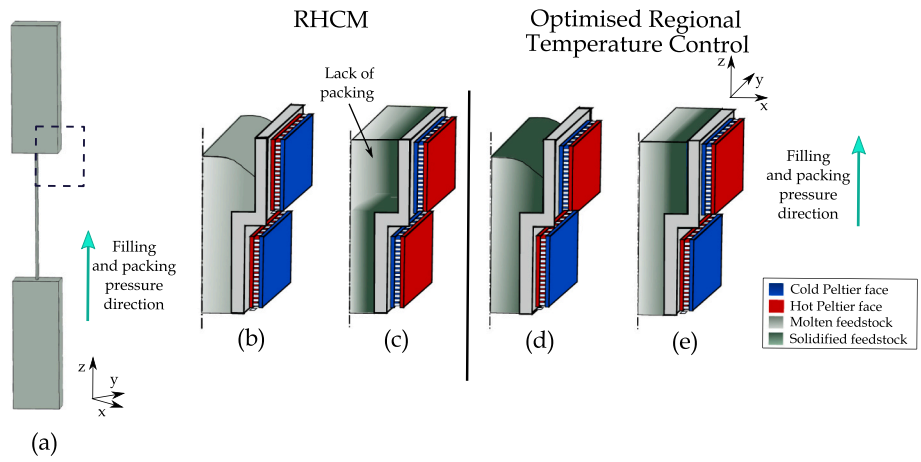

Fig. 16. Schematics of lack of packing during single sprue moulding with RHCM approach compared to the optimal case. (a) Schematics of the analysed sample and detailed of the magnified area. (b) Filling stage, RHCM. (c) Packing stage, RHCM. (d) Filling stage, optimised regional temperature control. (c) Packing stage, optimised regional temperature control.

Therefore, even more importantly than in the DS case, the simultaneous solidification of the inner portions of the features despite their differential thickness, promoted by the optimised solution, enables a more uniform shrinkage compensation within the part, as will be discussed more in depth in Section 5.2.

Moreover, upon cooling, the glass transition temperature of the material in the thin feature (Feature 2) is reached considerably faster than in the thick one, using the RHCM approach. Hence, the material within the component will undergo different undercooling times (T_{UC} in Fig. 15e-f): this will lead to a dissimilar development of the binder crystalline microstructure, which plays a fundamental role in shrinkage behaviour [28], as will be seen in Section 5.2.2.

The thermal model was validated through injection moulding experiments performed with the setup and materials described in Section 3, and a comparison between model and experimental results for the temperature profile inside the cavity at Feature 2 are presented in Fig. 17.

Since the employed mould did not have water-based cooling channels, higher limitations in heat dissipation on the heatsink side emerge compared to usual industrial moulds: this caused a lower efficiency of the system compared to the initially simulated one, implying that a slightly different heating and cooling profile had to be used for the trials. This explains the difference in temperature profiles comparing the results shown in Figs. 15 and 17. However, this did not constitute a limitation for the validation of the model and concept, as it implied a narrowing of the binding ranges for the time and temperature variables at the control points shown in Fig. 11, while similar cooling rates were achieved between thin and thick features in the optimal case and different ones using the RHCM approach.

As for cycle time considerations, no substantial difference can be detected between the regional temperature control approach and RHCM. This is due to the fact that, although keeping some cavity features at lower temperatures (as in the regional case) should decrease the required cooling time, heat transfer from warmer to colder areas of the cavity occurs, which prolongs cooling time. However, an enhanced insulation between mould features and an increased heat dissipation of the bolster side of the mould can be better achieved with water-based cooling channels.

5.2. *Characterisation of the thermal control approach effects on injection moulded parts*

As previously stated in Section 3, to validate the performance of the proposed mould temperature control approach, the already described thermal analysis is coupled with an investigation of macrostructural and microstructural properties of the components injected in this study. This analysis is divided into three parts: the first, discussing feature replication capability, followed by a study on the dimensional control of the injected parts and concluding with an analysis of both surface quality and weld lines.

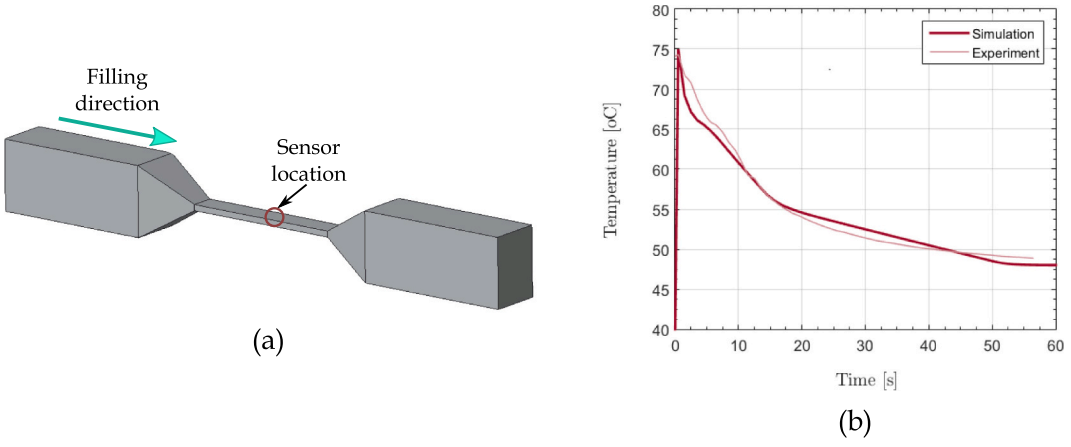

Fig. 17. Validation of the thermal control model: example for the Draft-part in SS configuration. (a) Schematics of the component. (b) Example temperature profile for model validation.

5.2.1. Feature replication capability

A sharp enhancement in feature replication capability was observed by increasing mould temperature corresponding to the thin channel (Feature 2) of the cavities (Fig. 18), showing that the local heating of the finest features is enough to ensure the complete injection of the components, without increasing the temperature of the whole mould.

In both the RHCM and optimised regional controlled cases, more than 100% flow length increase is observed with respect to the ambient temperature approach, leading to the achievement of complete filling of Step-part (Fig. 18b-c) when injected with double sprue configuration and of Draft-part (Fig. 18d-e) when injected in both single and double sprue configurations. The thinnest (0.5 mm) channel of Draft-part could not be fully filled with SS configuration, even using the RHCM approach, due to the high pressure drop in the channel and to the fact that feature thickness starts being comparable to particle size. This behaviour shows the effect of viscosity, which for the employed feedstock suddenly drops to values as low as approximately 2 Pa·sec at a temperature of 62 °C, with very low dependence on the shear rate: due to this, when mould temperature is kept constant (ambient) throughout the process, the material solidifies before reaching the end of the channel; differently, as the thinnest feature temperature is increased above the "viscosity drop" level, lower pressures and subsequent shear stresses are enough to fill the thinnest channels (Fig. 18a). This implies that the use of a higher pressure (around 25 bar if calculated through the Hagen-Poiseulle equation) would allow for the complete filling of the channel with a heated mould.

5.2.2. Dimensional control

One of the main advantages of the proposed regional control approach against the employment of a uniform mould temperature is related to the dimensional control of components moulded in SS configuration.

Shrinkage of the features located farther from the gate (i.e. Feature 1b, as shown in Fig. 19a) in the Draft-part, was measured for parts injected with the regional and RHCM approaches. Shrinkage was evaluated by placing the sample parts on a fixture and measuring, through the Alicona InfiniteFocus optical microscope, the relative heights and widths of Feature 1b injected with the RHCM and optimised regional control (Feature 1b, as shown in Fig. 19).

Results from these measurements (Table 2) show an average difference of approximately 50 μm in height (and thus in thickness, Δth) and of 130 μm in width (Δw), with the Feature 1b injected using the regional approach being larger and thicker than its equivalent injected using RHCM. Although the measured differences are quite low on an absolute value, the amount of shrinkage will drastically increase after the debinding and sintering processes. This negative effect has been proven

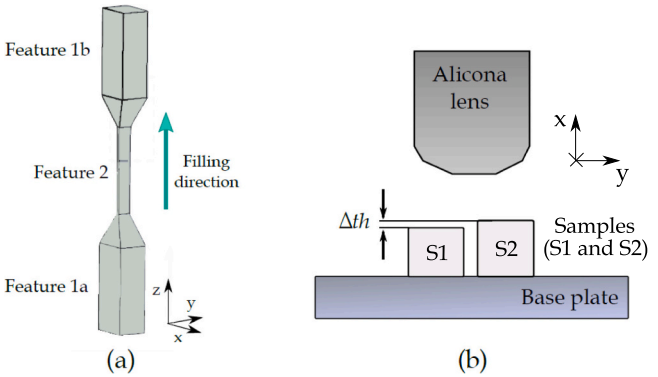

Fig. 19. Dimensional accuracy analysis (a) Schematics of the analysed sample features (b) Schematics of the setup for dimensional accuracy measurements, where S1 is the sample moulded using RHCM and S2 is the sample moulded using the regional temperature control approach.

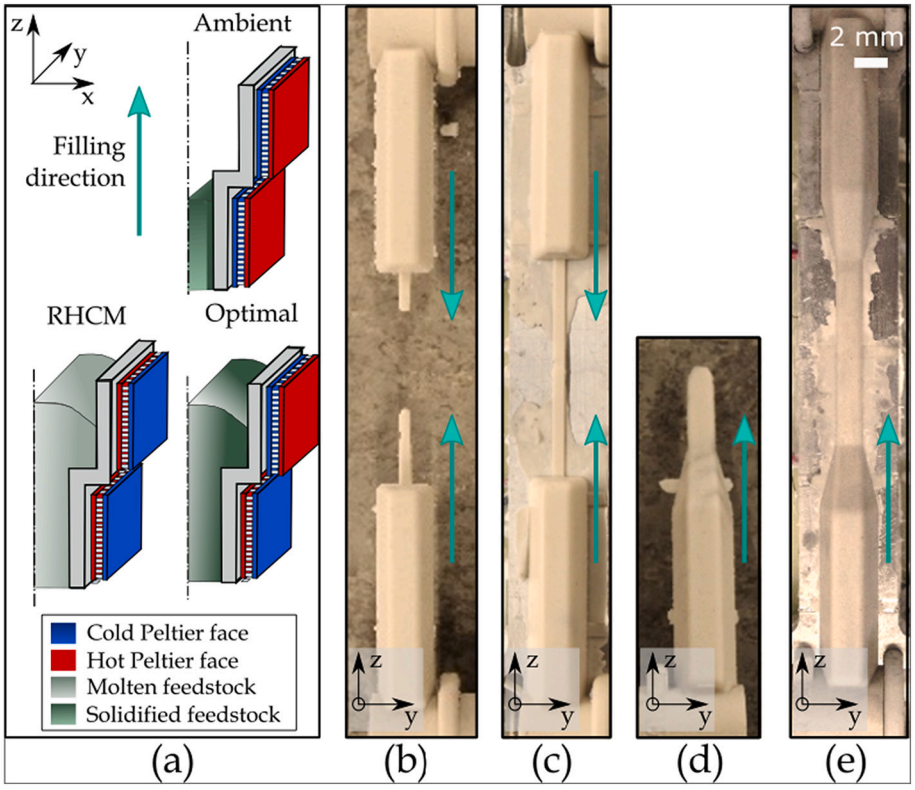

Fig. 18. Enhancement of feature replication capability using RHCM and regional control approach. (a) Schematics of temperature distribution and solidification profile during injection. (b) Step-part DS, $T_m = 35\ ^\circ C$. (c) Step-part DS, RHCM and optimal cases. (d) Draft-part SS, $T_m = 35\ ^\circ C$. (e) Draft-part SS, RHCM and optimal cases. Note: as the same flow length, during filling, was achieved in the RHCM and optical case, only one picture for both approaches is displayed for simplicity.

Table 2
Height difference among Feature 1 (farther from the gate) in the Draft-part, moulded in SS configuration. Average and standard deviation values calculated over three samples.

Shrinkage in moulded samples	
Average shrinkage (Feature 1a) [%]	1
Average shrinkage (Feature 1a) [μm]	125±21
Average Δth (Feature 1b) (regional - RHCM) [μm]	50
Average Δw (Feature 1b) (regional - RHCM) [μm]	130

to determine part warpage and cracking by studies analysing the evolution of defects through the debinding and sintering stages on CIM [29].

Moreover, this difference can be compared against a measured shrinkage of about 1%, implying an increase of linear shrinkage along the thickness direction of approximately 25% compared to Feature 1a.

The effect on shrinkage of the regional mould temperature approach, compared to the conventional RHCM, can be explained by looking at the compressible behaviour of the feedstock (Fig. 20).

In the RHCM case, during the filling stage, the material is molten and subjected to a higher pressure than atmospheric (Point 1-R in Fig. 20a-b), determining an increased specific volume of the feedstock (Fig. 20f), due to its high temperature. Once the cavity is fully filled, mould temperature is rapidly reduced uniformly, thus determining the quick solidification of the thinnest feature (as previously seen in the thermal analysis of Fig. 15g), while the material in the thicker portion of the cavity farthest from the gate (Feature 1b) is still in the molten state. On the other hand, in the optimised regional controlled mould temperature case, simultaneous cooling of the central portions of materials in the thin and thick part features occurs, leading to the solidification of the features farther from the gate at the imposed packing pressure (Point 1-O in Fig. 20d and f).

The effect of this solidification behaviour in the RHCM case is threefold: first, material shrinkage in Feature 1b during cooling will not be compensated, as no extra material will be fed into this portion of the cavity due to the freezing of the thinner feature, closer to the gate (Feature 2). Second, Feature 1a will cool without any applied packing pressure, causing a higher total specific volume variation compared to solidification with higher applied pressures (Fig. 20f): this is especially valid when high levels of packing pressure are used. Finally, in the cases of feedstocks having semi-crystalline binders, cooling rate causes a further variation of PVT behaviour of the material [30] due to the level of crystallinity obtained during undercooling. As a lower specific volume can be associated with a higher level of crystallinity [28], thin and thick sections will shrink differently in the RHCM case compared to the regional control approach, causing potential further stresses and warpage in the component.

It is anyway worth observing that allowing a full cavity cooling before ejection is fundamental to obtain such higher feature dimensional uniformity as, failing to do this may cause deformations in the components, as observed by Zhang and co-workers [31].

5.2.3. *Weld lines and surface quality*

Weld lines, created by the merging of multiple flow fronts of feedstock during mould filling, constitute weak areas on injected parts, as the poor blending of the different fronts determines the formation of a v-notch on the component surface where stress concentrates. Weld lines have been then analysed through SEM on the moulded samples, and a clear difference in their morphology can be observed when comparing components moulded using an ambient temperature and heated mould (both RHCM and optimal case). In the ambient mould temperature case, poor merging of the flow fronts is achieved (Fig. 21), due to higher viscosity of the feedstock material, approaching solidification, leading to a weld line approximately 100 μm below the top channel surface, as detected from (Fig. 21e). On the other hand, when the surface below the weld line area is heated during mould filling, proper merging of the flow fronts occurs, with no visible weld line appearing on the surface, even in the case of the thinnest feature of the Step-part (0.5 mm thick and 2 mm wide) as shown from SEM and Alicona measurements (Fig. 22d-e).

Analysing the samples at higher magnification (Fig. 22f), only a V-

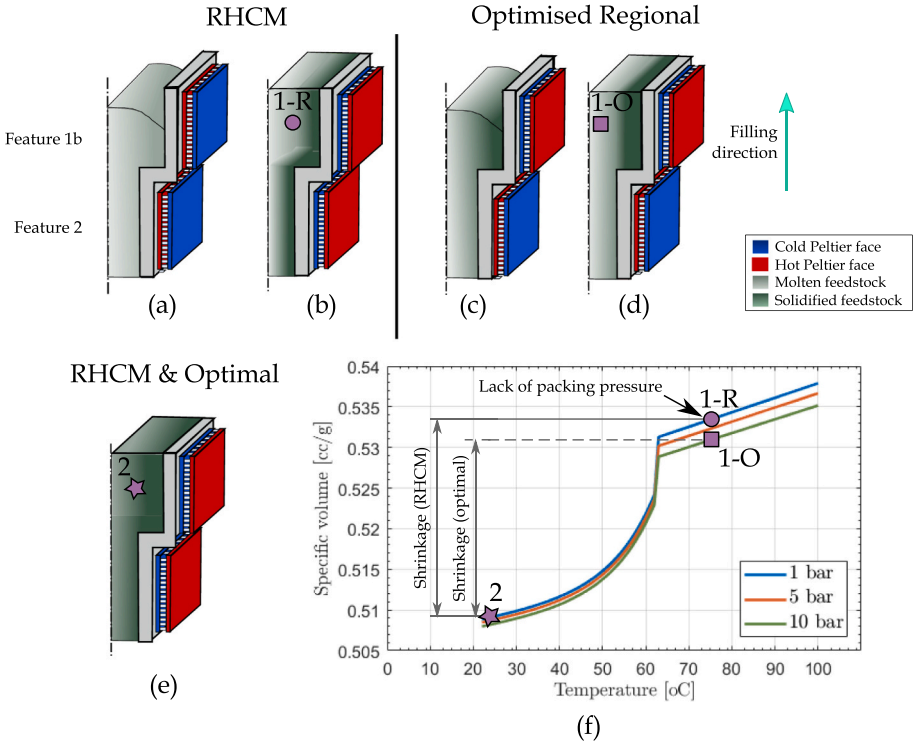

Fig. 20. CIM outcome: Dimensional control. (a) Schematics of mould filling, RHCM. (b) Schematics of the packing phase, RHCM. (c) Schematics of mould filling, optimal. (d) Schematics of the packing phase, optimal. (e) Schematic of the part after cooling, RHCM and optimal. (f) Example of PVT behaviour.

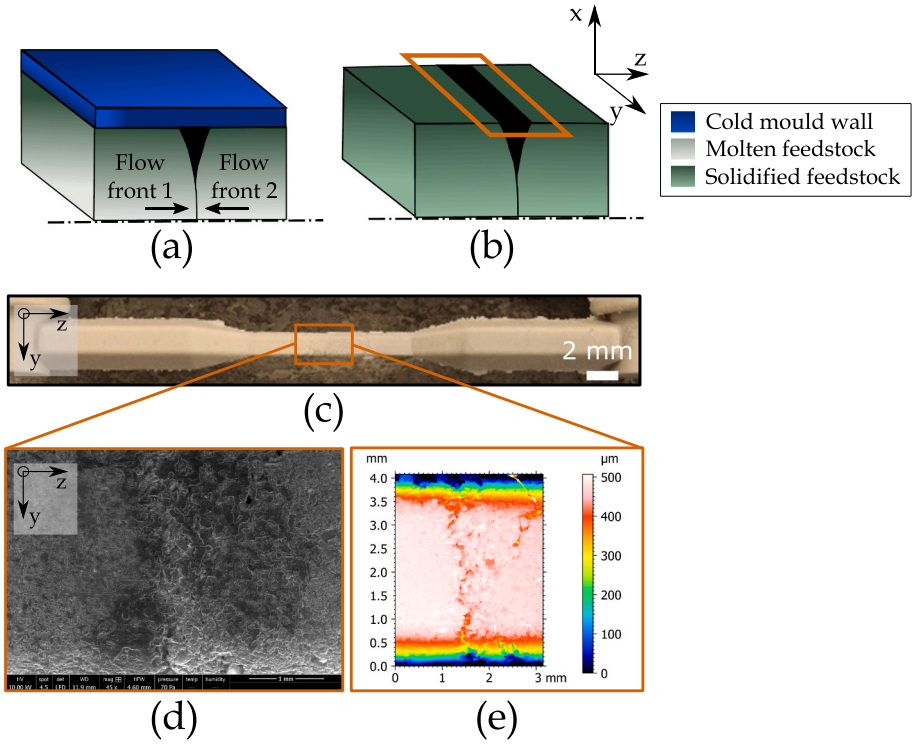

Fig. 21. CIM outcome: Weld lines in the ambient temperature case. (a) Schematics of weld lines creation, filling phase. (b) Schematics of weld lines, part after ejection. (c) Example of analysed component, Draft-part in DS configuration. (d) SEM micrograph of weld line. (e) Surface topography of weld line.

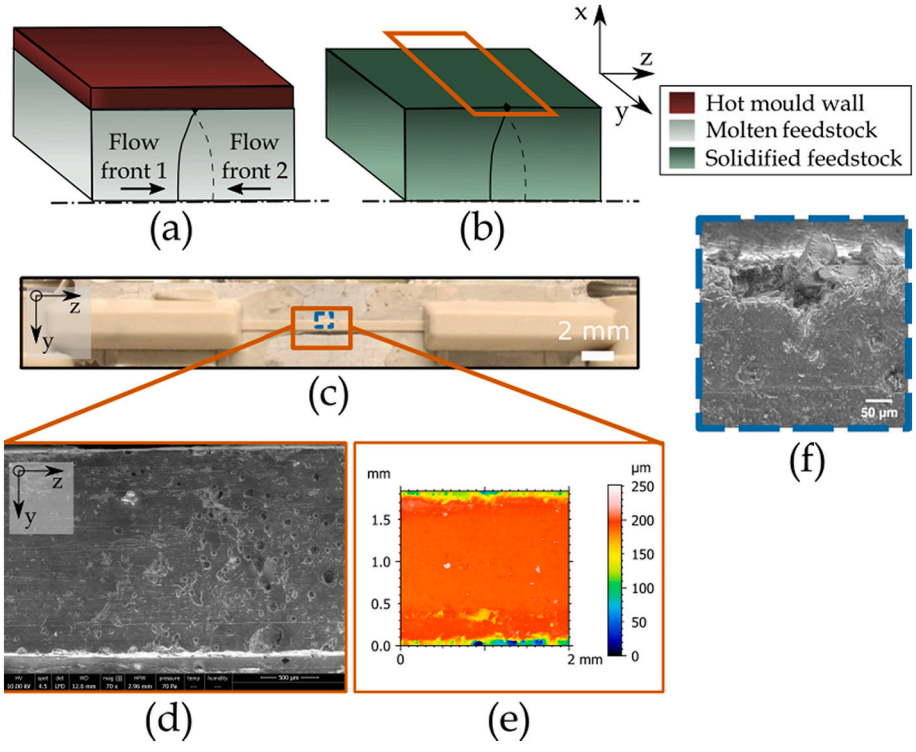

Fig. 22. CIM outcome: Weld lines in the regional optimised case. (a) Schematics of flow fronts merging, filling phase. (b) Schematics of the part with merged flow fronts, part after ejection. (c) Example of analysed component, Step-part in DS configuration. (d) SEM micrograph of weld line. (e) Surface topography of weld line. (f) SEM micrograph of the side of the top surface.

notch is visible on the side of the part: this is due to the local lower temperature on the side of the plates, not fully in contact with the Peltier modules. Considering this, while RHCM has been proved an effective technique to increase weld line strength in both unfilled and fibre-filled polymer injection moulding [20,32,19], both this technique and the regional increase of mould temperature at weld line locations lead to an

improvement in bonding of flow fronts at the component surface, implying a higher quality of green and subsequently sintered parts.

Considering surface quality, a clear distinction can be seen in the effect that different mould temperature approaches have on features having different thicknesses: in fact, when the components are injected using the isothermal (ambient) approach, the material flowing in thin channels is subjected to high shear rate levels, which are further increased by the rise in viscosity occurring due to feedstock solidification [21]. This causes the simultaneous formation of three orientation layers – frozen, shear and core – that can separate when the external frozen one solidifies (Fig. 23a-b). From the joint SEM-Alicona analysis it is possible to detect a 150 μm thick frozen layer, with a smoother top surface replicating mould cavity face; this separates from the underneath shear layer that is also richer of particles.

A smooth surface is instead replicated when injecting components increasing mould temperature under the thinnest feature, as previously shown in Fig. 22d-e. A difference on surface morphology can instead be detected when comparing the thick features moulded with RHCM and regional control methods (Fig. 24): a higher binder content is present on the surface of the component injected with RHCM (Fig. 24d), with ceramic particles enclosed within a top layer of wax-EVA blend.

In the regional temperature case, particles are instead directly exposed on the surface, which consequently exhibits a rougher morphology (Fig. 24d). This difference in surface quality is due to the effect of mould temperature on binder surface tension, which in the RHCM decreases, causing a higher wetting of both ceramic particles and mould cavity. When this phenomenon is coupled with high shear rate levels, separation of powder and binder occurs, which cases detrimental structural defects in moulded components. The effect of this difference in surface quality of sintered parts highly depends on geometrical tolerances of the components: in fact, while RHCM leads to a smoother surface on green components, the debinding process will cause the erosion of the external surface layer (richer of binder), hence causing potential inaccuracies in the main dimensions of the sintered parts.

6. Conclusions

The employment of suitable thermal control approaches is critical for the achievement of defect-free ceramic injection moulded components. Current approaches for mould heating and cooling have not been customised to enhance the capability of moulding components characterised by features having dissimilar wall thickness, which present strong challenges due to uneven cooling rates developing along the part. To overcome these limitations, a mould having a regional temperature control, achieved with the use of thermoelectric modules, was designed and manufactured. Moreover, a coupled PSO-FE thermal control model and optimisation was implemented and used to determine optimal Peltier temperature profiles with the objective of minimising the differences in cooling rates between different cavity features, despite their dissimilar wall thicknesses. To analyse the performance of the novel proposed approach, a thermal analysis was first carried out and then the effects of the considered approaches on moulded parts quality was studied. From this work, the following conclusions can be drawn:

- The thermal control model and optimisation allowed to find a solution consisting of a localised-RHCM technique in proximity of the thinnest cavity features: this approach has an enhanced performance when used on components having differential wall thickness, compared to state-of-the-art methods based on the achievement of uniform cavity temperature, as they cause uneven cooling rates in the part, which determine defects such as differential shrinkage and lack of packing in features far from the gate.
- The optimal regional temperature control approach provides a reduction up to 2-times in cooling rate differences between thin and thick features in the injected components. Moreover, it leads to simultaneous solidification of the material in the centre of the thin and thick areas of the cavity. This allows a more uniform shrinkage during solidification in parts with features of different thickness.
- The regional control method leads to comparable cycle times to the RHCM approach, reaching a total value of approximately 100 s with the employed setup. This gives a prospect of faster cycle times than the RHCM approach, when using the regional temperature control method with an industrial mould having water-based cooling channels.
- An enhancement in feature replication capability was achieved with the novel proposed method, comparable to a traditional RHCM

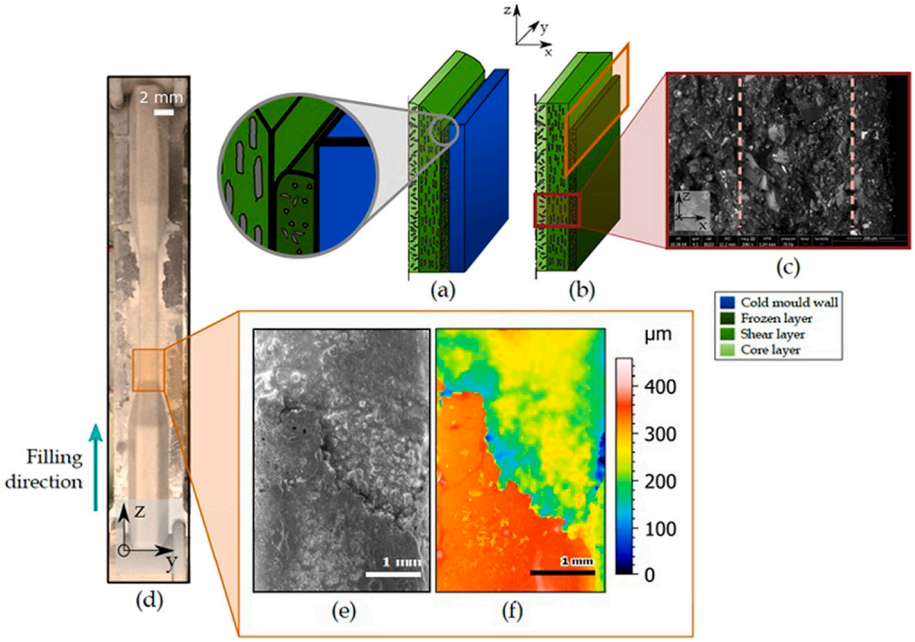

Fig. 23. CIM outcome: surface quality on the thin feature in the ambient temperature case. (a) Schematics of the particle orientation, filling phase. (b) Schematics of particle orientation, part after ejection. (c) SEM micrograph showing different orientation layers in the part cross section. (d) Example of analysed component, Draft-part in DS configuration. (e) SEM micrograph of shear-induced layer separation. (f) Surface topography of shear-induced layer separation.

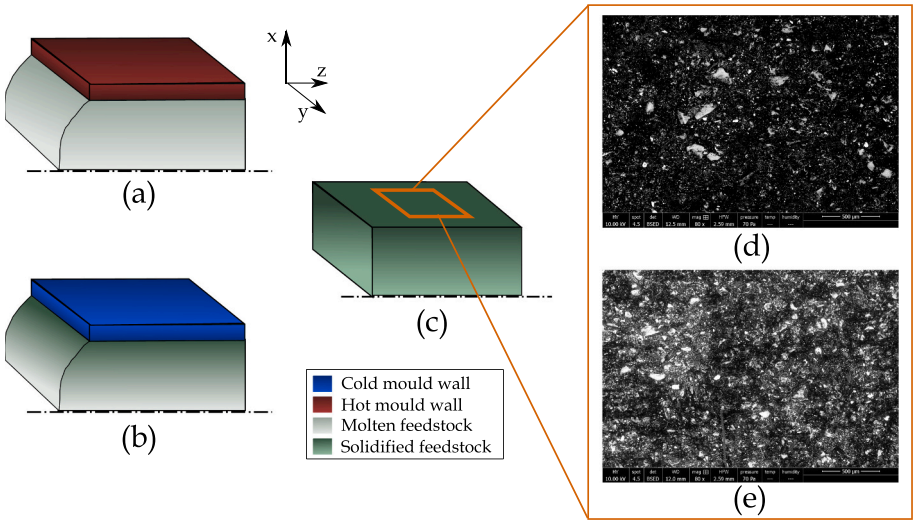

Fig. 24. CIM outcome: surface quality on the thick feature in the RHCM and regional control temperature cases. (a) Schematics of the phenomenon, filling phase, RHCM. (b) Schematics of the phenomenon, filling phase, regional optimised case. (c) Schematics of the phenomenon, part after ejection, with highlighted area of the surface. (d) SEM micrograph of feature surface, RHCM. (e) SEM micrograph of feature surface, regional optimised case.

approach and leading to a doubling in flow length for a channel having thickness of the order of 500 μm and width of 2 mm.

- Uniform packing and consequential improved dimensional control were achieved with the regional thermal control approach, as features at various locations from the gate did not exhibit significant dimensional differences. This is in contrast with the RHCM case, for which thick features far from the gate presented a further increase of approximately 25% in the volumetric shrinkage compared to those closer to the gate.
- The novel proposed method maintains the RHCM approach benefits in enhanced weld lines quality, and lack of shear-induced separation at the surface of thin features, while allowing higher solid loadings at the surface of thicker features. This will help preventing differential shrinkage and cracking defects during the sintering process.

This paper demonstrates that the use of uniform cooling rates during injection moulding, achieved with the novel proposed thermal control system, enhances the capability of manufacturing ceramic components with uneven wall thickness through CIM. This guarantees an increased flexibility in types and complexity of parts producible via CIM, which is especially relevant in high-value applications such as ceramic cores for the investment casting of turbine blades and vanes.

Declaration of competing interest

The authors declare that they have no known competing financial interests or personal relationships that could have appeared to influence the work reported in this paper.

Acknowledgements

The authors gratefully acknowledge the Nanoscale and Microscale Research Centre (NMRC) at the University of Nottingham for providing access to their facilities and equipment. This work was supported by the UK Engineering and Physical Sciences Research Council (EPSRC) under a Rolls-Royce CASE award scheme (EP/M507519/1).

References

[1] Sardarian M, Mirzaee O, Habibolahzadeh A. Numerical simulation and experimental investigation on jetting phenomenon in low pressure injection molding (LPIM) of alumina. J Mater Process Technol 2017;243:374–80.
[2] Baruffi Federico, Gülçür Mert, Calaon Matteo, Michel Romano Jean, Penchev Pavel, Dimov Stefan, Whiteside Ben, Tosello Guido. Correlating nano-scale surface replication accuracy and cavity temperature in micro-injection moulding using in-line process control and high-speed thermal imaging. J Manuf Process 2019;47:367–81.
[3] Surace Rossella, Bellantone Vincenzo, Trotta Gianluca, Fassi Irene. Replicating capability investigation of micro features in injection moulding process. J Manuf Process 2017;28:351–61.
[4] Wang Guilong, Zhao Guoqun, Li Huiping, Guan Yanjin. Research of thermal response simulation and mold structure optimization for rapid heat cycle molding processes, respectively, with steam heating and electric heating. Mater Des 2010;31(1):382–95.
[5] Xiao Cheng-Long, Huang Han-Xiong. Development of a rapid thermal cycling molding with electric heating and water impingement cooling for injection molding applications. Appl Therm Eng Dec 2014;73(1):712–22.
[6] Nian Shih-Chih, Huang Ming-Shyan, Tsai Tzung-Hung. Enhancement of induction heating efficiency on injection mold surface using a novel magnetic shielding method. Int Commun Heat Mass Transfer Jan 2014;50:52–60.
[7] Jeng Ming-Chang, Chen Shia-Chung, Minh Pham Son, Chang Jen-An, Chung Chia-shen. Rapid mold temperature control in injection molding by using steam heating. Int Commun Heat Mass Transfer Nov 2010;37(9):1295–304.
[8] Shayfull Z, Sharif S, Azlan Mohd. Zain MF Ghazali, Saad R Mohd. Potential of conformal cooling channels in rapid heat cycle molding: a review. Adv Polym Technol 2014;33(1). n/a|-n/a.
[9] Han Wei, Fang Fengzhou. Fundamental aspects and recent developments in electropolishing. Int J Mach Tool Manuf 2019;139:1–23.
[10] Zhang Jiong, Hao Wang A Senthil Kumar, Jin Mingsheng. Experimental and theoretical study of internal finishing by a novel magnetically driven polishing tool. Int J Mach Tool Manuf Jun 2020;153:103552.
[11] Finkeldey Felix, Volke Julia, Christoph Zarges Jan, Peter Heim Hans, Wiederkehr Petra. Learning quality characteristics for plastic injection molding processes using a combination of simulated and measured data. J Manuf Process 2020;60(April):134–43.
[12] Agazzi Alban, Sobotka Vincent, LeGoff Ronan, Jarny Yvon. Optimal cooling design in injection moulding process – a new approach based on morphological surfaces. Appl Therm Eng Apr 2013;52(1):170–8.
[13] Wang Guilong, Zhao Guoqun, Li Huiping, Guan Yanjin. Multi-objective optimization design of the heating/cooling channels of the steamheating rapid thermal response mold using particle swarm optimization. Int J Therm Sci 2011;50(5):790–802.
[14] Xiao Cheng-Long, Huang Han-Xiong. Optimal design of heating system for rapid thermal cycling mold using particle swarm optimization and finite element method. Appl Therm Eng 2014;64(1–2):462–70.
[15] Yiwei Dong, Xiaolin Li, Qi Zhao, Jun Yang, Ming Dao. Modeling of shrinkage during investment casting of thin-walled hollow turbine blades. J Mater Process Technol 2017;244:190–203.
[16] Kim Beomkeun, Min Juwon. Residual stress distributions and their influence on post-manufacturing deformation of injection-molded plastic parts. J Mater Process Technol Jul 2017;245:215–26.
[17] Kim Bwng H, Wadhwa Rajesh R. A new approach to low thermal inertia molding. Polym-Plast Technol Eng 1987;26(1):1–22.
[18] Nian Shih-Chih, Wu Chih-Yang, Huang Ming-Shyan. Warpage control of thin-walled injection molding using local mold temperatures. Int Commun Heat Mass Transfer 2015;61:102–10.

[19] Wang Xiaoxin, Zhao Guoqun, Wang Guilong. Research on the reduction of sink mark and warpage of the molded part in rapid heat cycle molding process. Mater Des 2013;47:779–92.
[20] Wang Guilong, Zhao Guoqun, Wang Xiaoxin. Effects of cavity surface temperature on mechanical properties of specimens with and without a weld line in rapid heat cycle molding. Mater Des Apr 2013;46:457–72.
[21] Bianchi Maria Floriana, Gameros Andrés A, Axinte Dragos A, Lowth Stewart, Cendrowicz Aleksander M, Welch Stewart T. On the effect of mould temperature on the orientation and packing of particles in ceramic injection moulding. J Eur Ceram Soc 2019;39(10):3194–207.
[22] Gromada Magdalena, Świeca Adam, Kostecki Marek, Olszyna Andrzej, Cygan Rafal. Ceramic cores for turbine blades via injection moulding. J Mater Process Technol 2015;220:107–12.
[23] Shengjie Y, Li QF, Yong MS. Method for determination of critical powder loading for powder-binder processing. Powder Metall 2006;49(3):219–23.
[24] Uematsu Keizo, Ohsaka Shigeru, Shinohara Nobuhiro, Okumiya Masataro. Grain-oriented microstructure of alumina ceramics made through the injection molding process. J Am Ceram Soc 1997;15(191539):1313–5.
[25] Nikolic Sasa, Randelovic Sasa, Milutinovic Mladomir. Effect of mold temperature on melt font temperature of thermoplastic resin at injection molding. J Technol Plasticity 2014;39(2).
[26] Zheng Rong, Tanner Roger I, Fan Xi-Jun. Injection molding: integration of theory and modeling methods. Springer; 2011.
[27] Somé Saannibe Ciryle, Delaunay Didier, Faraj Jalal, Bailleul Jean-Luc, Boyard Nicolas, Quilliet Stéphane. Modeling of the thermal contact resistance time evolution at polymer–mold interface during injection molding: effect of polymers' solidification. Appl Therm Eng 2015;84:150–7.
[28] Fischer Jerry M. Handbook of molded part shrinkage and warpage. William Andrew; 2013.
[29] Mannschatz Anne, Müller Axel, Moritz Tassilo. Influence of powder morphology on properties of ceramic injection moulding feedstocks. J Eur Ceram Soc Nov 2011;31 (14):2551–8.
[30] Zuidema H, Peters GWM, Meijer HEH. Influence of cooling rate on pVT-data of semicrystalline polymers. J Appl Polym Sci 2001;82(5):1170–86.
[31] Zhang Yang, Pedersen David Bue, Gótje Asger Segebrecht, Mischkot Michael, Tosello Guido. A soft tooling process chain employing additive manufacturing for injection molding of a 3D component with micro pillars. J Manuf Process 2017;27: 138–44.
[32] Wang Guilong, Zhao Guoqun, Wang Xiaoxin. Effects of cavity surface temperature on reinforced plastic part surface appearance in rapid heat cycle moulding. Mater Des Feb 2013;44:509–20.